Lukinović et al. Supplementary Information

SMYD3 impedes small cell lung cancer sensitivity to alkylation damage through RNF113A methylation-phosphorylation crosstalk

Supplementary Figure Legends

Supplementary Figure S1. SMYD3 is a candidate regulator of SCLC susceptibility to alkylating chemotherapy

A, Synthetic lethality screening using a library comprised of 285 characterized inhibitors, testing H209 SCLC cells sensitivity to cisplatin genotoxicity. Data represent relative growth of H209 cells treated with a combination of cisplatin (1 μM) and different inhibitors (1 μM each) compared to cisplatin alone. **B**, Analysis of normal human lung single-cell RNA sequencing data reveals low *SMYD3* expression in pulmonary neuroendocrine cells (PNEC); clusters of cell types are labeled; lung epithelial cell types in red (Human Lung Cell Atlas (41)). **C-H**, H209, H1092 and DMS-114 SCLC cell viability assays using different concentrations of either 4H-CP (C-E) or MMS (F-H) with or without SMYD3i (EPZ031686). Percentage of viable cells under each condition was normalized to untreated cells. *P-value* were calculated by two-way ANOVA with Tukey's testing for multiple comparisons. Data are represented as non-linear regression with mean ± SEM. **I**, Loewe synergy score calculated by SynergyFinder 2.0, with individual dose-response curves (left) and dose-response matrix (right) for 4H-CP and SMYD3i. **J**, Immunoblot analyses were performed

using the indicated antibodies with lysates of H1092 engineered cells used in xenograft assays presented in Figures 1F-H. Actin or Tubulin are shown as a loading control.

Supplementary Figure S2. Identification of RNF113A as a novel methylated substrate of SMYD3

A. *In vitro* methylation assay were performed using radiolabeled S-adenosylmethionine and recombinant RNF113A and SMYD3, with increasing concentrations of SMYD3 inhibitor (EPZ031686) at the indicated concentrations. Top panel, autoradiogram of methylation assay. Bottom panel, Coomassie stain of proteins in the reaction. **B**, Specific recognition of RNF113A K20me3 peptides by the anti- RNF113A-K20me3 antibody by dot blot analysis using the indicated biotinylated peptides. Streptavidin is shown as the loading control. **C**, Non-radiolabeled *in vitro* methylation assay using recombinant SMYD3 and RNF113A biotinylated peptides with different K20 methylation states as staring material. Methylation events are detected using dot blot and immunodetection by RNF113A K20me3 antibody. Streptavidin is shown as the loading control.

In all panels, representative of at least three independent experiments is shown unless stated otherwise. The numbers below the immunoblot lines represent the relative signal quantification (see also Supplemental Table 5).

Supplementary Figure S3. Characterization of RNF113A methylation in SCLC cell lines

A, Immunoblot analysis with the indicated antibodies of endogenous RNF113A K20me3 methylation following immunoprecipitation of total RNF113A from HeLa cells expressing doxycycline-inducible shRNA against SMYD3. Tubulin is shown as a loading control. **B**.

Immunodetection of RNF113A K20me3 following immunoprecipitation of stably expressed HA-RNF113A in HeLa cells after treatment with different concentrations of SMYD3i. Tubulin is shown as a loading control. **C**, Related to Figure 3D, validation of NAPY markers expressions (NEUROD1; ASCL1; POU2F3; YAP1) in classified SCLC subtypes of human lung cancer. Boxes represent 25th to 75th percentile, whiskers: 10% to 90%, center line: median. *P-value* were calculated by Kruskal-Wallis test. Analysis was performed using FPKM data for each specified gene obtained from NIHMS782739-Suppl_Table10 (34). NAPY SCLC subclassification was based on the original classification by Rudin et al., presented in NIHMS1023395-Supplementary_Table_1 (32).

D-E, Pearson correlation analyses of SMYD3 expression and SCLC cell lines resistance to cyclophosphamide (D, $\rho = 0.48$) and of EZH2 and SLFN11 expressions and SCLC cell lines resistance to platinum-based therapy (E, $\rho = 0.16$ and $\rho = -0.26$ respectively). The area under curve (AUC) was calculated by integration under the 16-point concentration-response curves, using the Broad Institute and NCI's Cancer Target Discovery and Development Network: Cancer Therapy Response Portal (CTRP). Pearson correlation coefficient (ρ) was calculated between gene expression and AUC.

F-G, Immunoblot analysis was performed with indicated antibodies using lysates of engineered DMS-114 cells (F) which were then used in cell survival assays using different concentrations of MMS (G). Percentage of living cells under each condition was normalized to untreated cells. *P-value* were calculated by two-way ANOVA with Tukey's testing for multiple comparisons. Data are represented as non-linear regression with mean ± SEM.

In all panels, representative of at least three independent experiments is shown unless stated otherwise. The numbers below the immunoblot lines represent the relative signal quantification (see also Supplemental Table 5).

Supplementary Figure S4. RNF113A is a phosphoprotein and its methylation repels the phosphatase PP4

A, Immunoblot analysis was performed with the indicated antibodies after co-immunoprecipitation of endogenous PPP4R3a from 293T cell extracts expressing HA-RNF113A WT, K20A or K20F mutants. **B**, Immunoblot analysis of RNF113A migration using engineered HeLa extracts with stable expression of RNF113A wildtype, S6A, N4, N5 and K20F mutants. Ku80 is shown as a loading control. **C**, Model of RNF113A regulation by the crosstalk of post-translational modifications induced by PP4 and SMYD3.

In all panels, representative of at least three independent experiments is shown unless stated otherwise. The numbers below the immunoblot lines represent the relative signal quantification (see also Supplemental Table 5).

Supplementary Figure S5. Methylation-phosphorylation crosstalk regulation of RNF113A impacts its E3 ligase activity

A, Immunoblot analysis was performed using the indicated antibodies with lysates of HeLa S3 engineered cells. Tubulin is shown as a loading control. **B**, Immunoblot analysis was performed with the indicated antibodies after *in vitro* E3 ubiquitin ligase activity assays using HA-RNF113A purified from HeLa S3 cells, with or without prior alkylating agent (MMS) treatment. ATP and E1/E2 enzymes were added as shown. **C**, Immunodetection

of auto-ubiquitinated RNF113A after TUBE (tandem ubiquitin binding element) pulldowns using H1048 SCLC cells extracts following treatment with 4H-CP. **D**, Immunoblot analysis was performed with the indicated antibodies after TUBE pulldowns from HeLa cells stably expressing RNF113A wildtype or catalytically inactive RNF113A ΔRING mutant, with or without MMS-induced alkylation damage. DNA damage marker γH2A.X is shown as a control of damage induction. **E**, Immunoblot analysis was performed with the indicated antibodies demonstrating RNF113A auto-ubiquitination after Ni-NTA pulldown from 293T cells with or without His-Ub ectopic expression and MMS treatment as shown. **F**, Cell survival assays using increasing concentrations of cisplatin in control and engineered DMS-114 SCLC cells with stable expression of SMYD3 and RNF113A. Percentage of living cells under each condition was normalized to untreated cells. *P-value* were calculated by two-way ANOVA with Tukey's testing for multiple comparisons. Data are represented as non-linear regression with mean ± SEM. **G**, Immunoblot analysis was performed with the indicated antibodies after TUBE pulldowns from HeLa cells stably expressing HA-RNF113A wildtype, S6A, N4 or N5 mutants, with or without MMS treatment. **H**, Immunoblot analysis was performed with the indicated antibodies after TUBE pulldowns from HeLa cells stably expressing HA-RNF113A wildtype or K20F mutant, with or without MMS treatment. **I**, Immunoblot analysis was performed with the indicated antibodies using HeLa cells stably expressing either RNF113A wildtype or K20F mutant, with or without MMS treatment. **J**, Immunoblot analysis of auto-ubiquitinated RNF113A after Ni-NTA pulldown from 293T cells with ectopic expression of His-Ub, HA-RNF113A wildtype or K20F mutant and MMS treatment; where indicated. **K**, Immunoblot analysis was performed with the indicated antibodies after TUBE pulldowns from HeLa

cells stably expressing HA-RNF113A wildtype, K20F, N5 or K20F/N5 mutants, with or without MMS treatment.

In all panels, representative of at least three independent experiments is shown unless stated otherwise. The numbers below the immunoblot lines represent the relative signal quantification (see also Supplemental Table 5).

Supplementary Figure S6 (related to Figure 6). RNF113A regulation impacts its function in DNA dealkylation repair

A, Immunoblot analysis with indicated antibodies for comparison of SMYD3 and RNF113A expression levels in HeLa, U20S and H1048 SCLC cells. **B**, Immunoblot analysis was performed using the indicated antibodies with lysates of U2OS cells expressing the indicated vectors. **C**, Immunoblot analysis was performed as in (G) using lysates of U2OS cells expressing the indicated vectors. **D**, Immunoblot analysis of shRNA control (shControl) or shRNA RNF113A knockdown (shRNF113A) in U2OS cells. GAPDH is shown as a loading control. **E**, Representative images of MMS-induced ASCC3 foci in U2OS cells reconstituted with either RNF113A wildtype, S6A or N5 mutants after shRNA knockdown of endogenous RNF113A. Foci were monitored by immunofluorescent staining of ASCC3 (left panels) and the DNA damage marker γH2A.X (right panels). **F**, Quantification of U2OS cells from (E) with five or more MMS-induced ASCC3 foci. At least 100 cells were counted for each experimental condition. *P-value* were calculated by two-tailed unpaired Student's t test, error bars represent mean ± SD. **G**, Representative images of immunofluorescent staining signal intensity of MMS-induced ASCC3 foci in U2OS cells related to Figure 4D. **H**, Quantification of immunofluorescent staining signal

intensity of individual ASCC3 foci from RNF113A wildtype (n = 26 foci) and RNF113A K20F mutant (n = 18 foci) expressing U2OS cells as shown in (G). *P-value* were calculated by two-tailed unpaired Student's t test, error bars represent mean ± SEM. **I-J**, Cell survival assays with the indicated concentrations of MMS in HeLa cells with or without SMYD3i (I) or in engineered HeLa cells stably expressing either control vector, RNF113A WT or K20F mutant (J). Percentage of living cells under each condition was normalized to untreated cells. *P-value* were calculated by two-way ANOVA with Tukey's testing for multiple comparisons. Data are represented as non-linear regression of the mean ± SEM.

In all panels, representative of at least three independent experiments is shown unless stated otherwise.

Supplementary Figure S7. SMYD3 inhibition sensitizes SCLC to alkylating agents *in vivo*

A, Schematic of the SCLC mouse model that recapitulates canonical genetic alterations that co-occur in human disease. The triple knockout (TKO) model was generated by breeding mice that carry conditional deletion of $Rb1^{LoxP/LoxP}$, $Rbl2^{LoxP/LoxP}$ and $Tp53^{LoxP/LoxP}$. Tumorigenesis in mice is induced by intratracheal installation of adenovirus expressing Cre-recombinase (Ad-Cre). **B**, Representative IHC staining of normal lung tissue and TKO and RPM ($Rb^{LoxP/LoxP};p53^{LoxP/LoxP};H11^{LSL\text{-}MycT58A}$) SCLC mouse models (representative of n = 12 samples for each group). Of note all analyzed *TKO* and *RPM* samples showed nuclear and cytoplasmic SMYD3 expression with H-score >150. Tumors in *TKO;Smyd3* mutant mice were negative for SMYD3 expression which confirms correct Cre-recombination of mutant allele. Scale bars, 50 µm. **C**, *Smyd3* expression in wildtype lung and *TKO* tumor samples by RTq-PCR, n = 12 samples for each group. *P-values* were

calculated by two-tailed unpaired t-test. **D,** Schematic of the *Smyd3* conditional allele. In the presence of Cre recombinase, exon 2 is deleted to disrupt *Smyd3* expression. **E**, Immunoblot analysis with the indicated antibodies of lysates from *Smyd3*$^{LoxP/LoxP}$ lung fibroblasts transduced with Ad-Cre or vehicle (control). Tubulin is shown as a loading control. **F**, Immunoblot analysis with the indicated antibodies of tumor biopsy lysates from *TKO and TKO;Smyd3* mutant mice treated with cyclophosphamide (CP) or vehicle (control). Two independent and representative samples are shown for each condition. Tubulin is shown as a loading control.

Supplementary Figure S8. SMYD3 inhibition sensitizes SCLC PDX to alkylating agents.

A, Representative H&E and IHC staining for cell proliferation marker phospho-histone 3 (pH3) and apoptosis maker cleaved Caspase 3 (cl. Caspase 3) in biopsies collected from therapy naïve SCLC patient derived xenografts (PDX-1) treated with SMYD3 inhibitor EPZ031686 (SMYD3i) and cyclophosphamide (CP). Representative of n = 6 mice for each experimental group. Scale bars, 50 µm. **B-C**, Quantification of phospho-Histone 3 (pH3) (B) and cleaved Caspase 3 (cl. Caspase 3) positive cells (C) in PDX samples as in (A). Boxes represent 25th to 75th percentile, whiskers: min. to max., center line: median; *P-value* were calculated by two-way ANOVA with Tukey's testing for multiple comparisons. **D**, Weight analysis over time of mouse groups from the PDX-1 study. **E**, Representative H&E and IHC staining for cell proliferation marker phospho-histone 3 (pH3) and apoptosis maker cleaved Caspase 3 (cl. Caspase 3) in biopsies collected from chemotherapy (Carboplatin and Etoposide) relapsed SCLC patient-derived xenografts (PDX-2) treated with SMYD3 inhibitor EPZ031686 (SMYD3i) and cyclophosphamide (CP). Representative

of n = 6 mice for each experimental group. Scale bars, 50 µm. **F-G**, Quantification of phospho-Histone 3 (pH3) (F) and cleaved Caspase 3 (cl. Caspase 3) positive cells (G) in PDX samples as in (E). Boxes represent 25th to 75th percentile, whiskers: min. to max., center line: median; *P-value* were calculated by two-way ANOVA with Tukey's testing for multiple comparisons. **H**, Weight analysis over time of mouse groups from the PDX-2 study.

Supplementary Tables

Supplementary Table S1. List of compounds used in cell growth inhibition screen with 4-hydroperoxy-cyclophosphamide (4H-CP) and cisplatin. Data represents ratio of 4H-CP or cisplatin to DMSO cell growth ± SD.

Compound	Supplier	Relative growth 4H-CP / DMSO	SD	Relative growth Cisplatin / DMSO	SD	Target
Niraparib	Selleckchem	0.322	0.004	0.451	0.015	PARP
EPZ031686	MedChemExpress	0.334	0.008	0.905	0.003	SMYD3
CM10	Selleckchem	0.344	0.004	0.788	0.002	Aldehyde dehydrogenase 1A family
NU1025	Selleckchem	0.357	0.005	0.525	0.003	PARP
EPZ030456	SGC	0.394	0.003	0.849	0.011	SMYD3
KU-60019	Selleckchem	0.416	0.006	0.903	0.011	ATM
5-Aza-2′-deoxycytidine	Sigma	0.431	0.003	0.417	0.002	5 aza 2 deoxycytidine
Buthionine sulfoximine (BSO)	Selleckchem	0.432	0.004	0.677	0.001	Glutathione (GSH) synthesis
AZD6738	Selleckchem	0.474	0.004	0.494	0.004	ATR
Etoposide	Selleckchem	0.495	0.004	0.560	0.016	DNA topoisomerase II
Pemetrexed Disodium	Selleckchem	0.523	0.003	0.647	0.006	Antifolate and antimetabolite
AZD7762	Selleckchem	0.535	0.005	0.404	0.012	Chk1/2
BAY-876	Selleckchem	0.562	0.003	0.712	0.004	GLUT1
NU7441 (KU-57788)	Selleckchem	0.598	0.004	0.445	0.008	DNA-PK inhibitor
J4	Selleckchem	0.609	0.007	0.568	0.016	JMJD3 and UTX
Topotecan	Selleckchem	0.656	0.003	0.562	0.013	Topoisomerase I
GSK690693	Selleckchem	0.720	0.005	0.805	0.013	Akt1, Akt2 and Akt3
Decitabine	Selleckchem	0.728	0.007	0.660	0.016	DNA methyltransferases
A-366	Selleckchem	0.754	0.007	0.711	0.006	G9a/GLP
Dinaciclib (SCH727965)	Selleckchem	0.756	0.012	0.648	0.010	CDK2, CDK5, CDK1 and CDK9
CFI-400945	Selleckchem	0.784	0.001	0.667	0.001	Plk4
RGFP966	Selleckchem	0.784	0.010	0.749	0.004	HDAC3i
SGC2085	Selleckchem	0.789	0.001	0.510	0.010	CARM1
JQ1	Selleckchem	0.794	0.007	0.678	0.006	BETi bromodomain
EPZ-6438	Selleckchem	0.806	0.009	0.409	0.004	EZH2
LDC4297 (LDC044297)	Selleckchem	0.815	0.004	0.870	0.001	CDK7
Trichostatin A	Sigma-Aldrich	0.829	0.011	1.260	0.016	HDACs

Paclitaxel	Selleckchem	0.834	0.001	0.671	0.014	Microtubule polymer stabilizer
UNC0638	Selleckchem	0.844	0.004	0.704	0.010	G9a/GLP
OTSSP167	Selleckchem	0.854	0.008	0.782	0.013	MELK
EPZ015666 (GSK3235025)	Selleckchem	0.869	0.005	0.832	0.003	PRMT5
Ganetespib (STA-9090)	Selleckchem	0.878	0.010	0.890	0.002	Hsp90
Fingolimod (FTY720)	Selleckchem	0.882	0.007	0.982	0.004	S1P receptor agonist
Doxorubicin	Selleckchem	0.894	0.004	0.867	0.007	DNA topoisomerase II
PF-3758309	Selleckchem	0.905	0.003	0.881	0.015	PAK
Omipalisib (GSK2126458)	Selleckchem	0.906	0.012	0.890	0.001	p110α/β/δ/γ, mTORC1/2
Capecitabine	Selleckchem	0.907	0.011	0.778	0.008	Prodrug of 5-fluorouracil
Afatinib (BIBW2992)	Selleckchem	0.909	0.014	0.983	0.006	EGFR/HER2
SIS3 HCl	Selleckchem	0.910	0.016	0.987	0.006	Smad3
PAC-1	Selleckchem	0.915	0.001	0.562	0.013	Procaspase-3 activator
Ponatinib (AP24534)	Selleckchem	0.917	0.006	0.863	0.013	Multi-target kinase inhibitor
NMS-873	Selleckchem	0.920	0.016	0.994	0.006	p97
Autophinib	Selleckchem	0.921	0.014	0.923	0.001	Autophagy
Trametinib (GSK1120212)	Selleckchem	0.927	0.009	0.888	0.005	MEK1/2
BI-847325	Selleckchem	0.935	0.001	0.865	0.005	Dual MEK1/2 and Aurora
Dabrafenib (GSK2118436)	Selleckchem	0.943	0.013	0.886	0.016	BRAF-V600
OTS964	Selleckchem	0.951	0.007	0.975	0.003	TOPK
Cisplatin	Selleckchem	0.957	0.012	N/A	N/A	DNA adduct
NSC 319726	Selleckchem	0.959	0.006	1.004	0.011	p53(R175) mutant reactivator
YU238259	Selleckchem	0.962	0.008	0.869	0.003	Homology-dependent DNA repair
Streptozotocin (STZ)	Selleckchem	0.963	0.008	1.034	0.005	Streptozotocin
NCB-0846	Selleckchem	0.968	0.007	0.992	0.004	TNIK
SB202190 (FHPI)	Selleckchem	0.973	0.011	1.007	0.007	p38α/β
Tanzisertib(CC-930)	Selleckchem	0.973	0.014	0.863	0.004	JNK
Telmisartan	Selleckchem	0.974	0.001	1.041	0.014	Angiotensin II receptor antagonist
Temozolomide	Selleckchem	0.974	0.006	1.072	0.013	Alkylates and cross-links DNA
Vismodegib (GDC-0449)	Selleckchem	0.975	0.007	1.291	0.015	Hedgehog
DDR1 Inhibitor	Sigma-Aldrich	0.976	0.013	0.566	0.017	DDR1/2
BAY598	Bayer	0.977	0.011	0.971	0.016	SMYD2
LY2584702	Selleckchem	0.980	0.007	0.989	0.004	p70S6K
Lifirafenib (BGB-283)	Selleckchem	0.981	0.009	0.921	0.004	RAF family kinases and EGFR
Oltipraz	Selleckchem	0.981	0.011	0.980	0.011	Nrf2 activator
GW0742	Selleckchem	0.981	0.021	0.942	0.003	PPARβ/δ agonist

Vorasidenib (AG-881)	Selleckchem	0.981	0.010	0.965	0.008	IDH1 and IDH2
Chloroquine Phosphate	SCBT	0.982	0.011	0.870	0.009	Autophagy
Ruxolitinib (INCB018424)	Selleckchem	0.983	0.002	0.930	0.016	JAK1/2
AS2444697	Sigma-Aldrich	0.983	0.002	0.985	0.003	IRAK4
HJC0152	Selleckchem	0.983	0.008	0.991	0.011	Stat3
PX-12	Selleckchem	0.983	0.008	1.039	0.011	Thioredoxin-1 (Trx-1)
Tianeptine sodium	Selleckchem	0.983	0.002	1.061	0.017	Serotonin reuptake enhancer
APS-2-79	Selleckchem	0.983	0.010	0.896	0.004	RAF
NSC87877	Selleckchem	0.983	0.008	0.917	0.006	SHP-1 and SHP-2
AZD7545	Selleckchem	0.983	0.010	0.970	0.005	PDHK
A-196	Selleckchem	0.983	0.010	1.049	0.004	SUV420H1 and SUV420H2
CA-4948	Selleckchem	0.984	0.008	0.885	0.016	IRAK4
TG003	Selleckchem	0.984	0.011	1.011	0.006	Cdc2-like kinase (Clk)
CHIR-99021	Selleckchem	0.985	0.012	0.790	0.012	GSK-3α and GSK-3β
GSK2801	Selleckchem	0.985	0.011	0.888	0.006	Bromodomains BAZ2A/B
Salirasib (FTS)	Selleckchem	0.985	0.012	0.992	0.003	Prenylated protein methyltransferase
K02288	Selleckchem	0.985	0.009	1.098	0.015	ALK2, ALK1 , ALK3 and ALK6
Enzastaurin (LY317615)	Selleckchem	0.985	0.006	0.940	0.011	PKCβ
PFI-2 HCl	Selleckchem	0.985	0.004	0.965	0.013	SETD7
BIBR 1532	Selleckchem	0.985	0.011	0.981	0.009	Telomerase
Pevonedistat (MLN4924)	Selleckchem	0.986	0.008	0.984	0.014	Nedd8 activating enzyme (NAE)
WNK463	Selleckchem	0.986	0.006	0.986	0.002	pan-WNK-kinase
Reparixin (Repertaxin)	Selleckchem	0.986	0.015	0.991	0.004	CXCR1/R2
SRPIN340	Selleckchem	0.986	0.013	0.991	0.008	SRPK
Pirfenidone	Selleckchem	0.986	0.011	0.848	0.013	TGF-β
LB-100	Selleckchem	0.986	0.006	0.906	0.013	PP2A
Quizartinib (AC220)	Selleckchem	0.986	0.008	0.991	0.005	FLT3
NVP-BHG712	Selleckchem	0.987	0.008	0.965	0.009	EphB4
iCRT3	Selleckchem	0.987	0.008	0.992	0.013	Antagonist of Wnt/β-catenin
Idasanutlin (RG-7388)	Selleckchem	0.987	0.011	1.002	0.015	p53-MDM2 interaction
BIX 02189	Selleckchem	0.987	0.011	1.035	0.013	MEK5 and ERK5
TH287	Selleckchem	0.987	0.006	1.089	0.004	MTH1 (NUDT1)
COTI-2	Selleckchem	0.987	0.014	0.903	0.016	Activator of mutant p53
LGK-974	Selleckchem	0.987	0.010	0.930	0.016	PORCN
Salubrinal	Selleckchem	0.987	0.007	0.970	0.004	eIF2α
LDC1267	Selleckchem	0.987	0.011	0.983	0.001	Mer, Tyro3, and Axl
Birinapant	Selleckchem	0.987	0.007	0.985	0.011	SMAC mimetic antagonist

Resiquimod	Selleckchem	0.987	0.007	1.001	0.015	TLR 7/8 agonist
Navitoclax (ABT-263)	Selleckchem	0.988	0.006	0.893	0.001	Bcl-xL, Bcl-2 and Bcl-w
BI-9564	Selleckchem	0.988	0.002	0.906	0.001	BRD9 and BRD7 bromodomains
UNC0379	Selleckchem	0.988	0.004	1.011	0.006	SETD8
LY2409881	Selleckchem	0.988	0.007	0.975	0.016	IKK2
PYR-41	Selleckchem	0.988	0.003	0.978	0.015	Ubiquitin-activating enzyme E1
LDC000067	Selleckchem	0.988	0.008	0.993	0.001	CDK9
STF-62247	Selleckchem	0.988	0.013	0.999	0.004	Inhibitor of renal cells lacking VHL
Lonidamine	Selleckchem	0.988	0.003	1.012	0.013	Hexokinase
Tasisulam (LY573636)	Selleckchem	0.989	0.001	0.763	0.007	Apoptosis inducer
Montelukast	Selleckchem	0.989	0.006	0.956	0.011	Leukotriene D 4 (LTD4) antagonist
CC-292 (AVL-292)	Selleckchem	0.989	0.008	1.080	0.002	BTK
YM155	Selleckchem	0.989	0.005	1.201	0.008	Survivin promoter
Diacerein	Selleckchem	0.989	0.007	0.963	0.002	Interleukin-1B (IL-1B)
EPZ020411	Selleckchem	0.989	0.011	0.984	0.005	PRMT6
Sonidegib (NVP-LDE225)	Selleckchem	0.989	0.013	0.989	0.015	Smoothened (Smo) antagonist
AT13148	Selleckchem	0.989	0.004	0.990	0.003	Multi-AGC kinase inhibitor
PF 670462	Sigma-Aldrich	0.989	0.011	1.013	0.016	Casein kinase 1ε and 1δ
AZD3965	Selleckchem	0.989	0.001	1.284	0.005	Monocarboxylate transporter
S63845	Selleckchem	0.990	0.002	0.716	0.007	MCL1
AMD3465 hexahydrobromide	Selleckchem	0.990	0.001	1.038	0.004	CXCR4 antagonist
KRpep-2d	Selleckchem	0.990	0.011	1.080	0.006	K-Ras(G12D)
LY3039478	Selleckchem	0.990	0.002	1.104	0.005	Notch cleavage inhibitor
Pioglitazone	Selleckchem	0.990	0.007	0.912	0.013	PPARγ agonist
Ispinesib (SB-715992)	Selleckchem	0.990	0.006	0.981	0.014	Kinesin spindle protein (KSP)
BI-D1870	Selleckchem	0.990	0.008	0.988	0.013	RSK1/2/3/4
SF1670	Selleckchem	0.990	0.001	1.005	0.010	PTEN
Desloratadine	Selleckchem	0.990	0.001	1.117	0.001	Histamine H1 receptor antagonist
10058-F4	Selleckchem	0.991	0.006	0.795	0.003	c-Myc
Ipatasertib (GDC-0068)	Selleckchem	0.991	0.009	0.846	0.013	Akt1, Akt2, and Akt3
Dovitinib	Selleckchem	0.991	0.008	0.906	0.008	Multi-targeted RTK inhibitor
Momelotinib (CYT387)	Selleckchem	0.991	0.005	0.911	0.006	TBK1, JAK1/JAK2
Nintedanib (BIBF 1120)	Selleckchem	0.991	0.005	0.983	0.014	VEGFR, FGFR1/2/3,PDGFRα/β
Triptolide (PG490)	Selleckchem	0.991	0.009	1.013	0.006	NF-κB
BI665915	Boehringer Ingelheim	0.991	0.009	1.037	0.006	FLAP
WZ811	Selleckchem	0.991	0.011	0.916	0.003	CXCR4 antagonist
ML323	Selleckchem	0.991	0.006	0.963	0.012	USP1/UAF1

Isoprenaline HCl	Selleckchem	0.991	0.013	0.975	0.005	β-adrenergic receptor agonist
GSK583	Selleckchem	0.991	0.007	1.004	0.011	RIP2
XAV-939	Selleckchem	0.991	0.001	1.013	0.007	Tankyrase1/2
Deltarasin	Selleckchem	0.991	0.001	1.173	0.002	KRAS-PDEδ interaction
Irinotecan	Selleckchem	0.992	0.005	0.408	0.009	Topoisomerase I
SGC-CBP30	Selleckchem	0.992	0.006	0.863	0.013	CREBBP/EP300
XL413 (BMS-863233)	Selleckchem	0.992	0.001	0.937	0.006	CDC7
CPI-613	Selleckchem	0.992	0.012	0.973	0.014	Pyruvate dehydrogenase
GNF-6231	Selleckchem	0.992	0.004	0.977	0.013	Porcupine
Galunisertib (LY2157299)	Selleckchem	0.992	0.006	0.984	0.006	TGFβ receptor I
Necrosulfonamide	Selleckchem	0.992	0.002	1.013	0.006	MLKL
MK-1775	Selleckchem	0.992	0.006	1.311	0.015	Wee1
EHT 1864	Selleckchem	0.992	0.003	0.866	0.011	Rac1, Rac1b, Rac2 and Rac3
PFI-3	Selleckchem	0.992	0.013	0.944	0.014	SMARCA bromodomain inhibitor
HA15	Selleckchem	0.992	0.008	0.963	0.011	BiP/GRP78/HSPA5
LTX-315	Selleckchem	0.992	0.001	0.964	0.011	Bax/Bak-oncolytic peptide
CB-839	Selleckchem	0.992	0.003	0.970	0.007	Glutaminase
AZ191	Selleckchem	0.992	0.001	0.975	0.004	DYRK1B
CCG-203971	Sigma-Aldrich	0.992	0.013	0.978	0.001	Rho/MKL1/SRF
Tofacitinib (CP-690550)	Selleckchem	0.992	0.004	1.003	0.006	JAK3
GSK2334470	Selleckchem	0.992	0.004	1.014	0.008	PDK1
BI639667	Boehringer Ingelheim	0.992	0.007	1.085	0.003	CCR1 antagonist
Pazopanib	Selleckchem	0.993	0.006	0.878	0.006	Multi-target kinase inhibitor
Regorafenib	Selleckchem	0.993	0.005	0.887	0.006	KIT, PDGFRβ, RAF, RET, VEGFR
GSK2830371	Selleckchem	0.993	0.005	0.954	0.005	Wip1 phosphatase
Super-TDU	Selleckchem	0.993	0.006	0.966	0.008	YAP-TEAD inhibitory peptide
4EGI-1	Selleckchem	0.993	0.005	0.970	0.002	eIF4E/eIF4G interaction
ROC-325	Selleckchem	0.993	0.006	1.010	0.006	Lysosomal-mediated autophagy
Tiplaxtinin (PAI-039)	Selleckchem	0.993	0.001	0.959	0.004	PAI-1
Metformin	Sigma-Aldrich	0.993	0.007	0.979	0.017	AMPK activator
OICR-9429	Selleckchem	0.993	0.003	0.986	0.011	Antagonist of WDR5-MLL-Histone 3
PFK15	Selleckchem	0.993	0.006	0.988	0.008	6-phosphofructo-2-kinase (PFKFB3)
PRI-724	Selleckchem	0.993	0.003	0.989	0.012	Wnt signaling
SGC707	Selleckchem	0.993	0.008	1.004	0.015	PRMT3
Liproxstatin-1	Selleckchem	0.993	0.003	1.203	0.016	Ferroptosis inhibitor
Pinometostat (EPZ5676)	Selleckchem	0.994	0.004	0.808	0.008	DOT1L
GSK1904529A	Selleckchem	0.994	0.004	0.868	0.016	IGF-1R and IR

AZD1208	Selleckchem	0.994	0.004	0.890	0.011	Pim1, Pim2, and Pim3
C646	Selleckchem	0.994	0.006	0.984	0.011	p300 histone acetyltransferase
GSK2656157	Selleckchem	0.994	0.008	1.089	0.017	PERK
EED226	Selleckchem	0.994	0.003	0.605	0.013	PRC2
Triapine	Selleckchem	0.994	0.001	0.981	0.017	Ribonucleotide reductase inhibitor
PNU-74654	Selleckchem	0.995	0.005	1.003	0.012	β-catenin and Tcf4 interaction
Sunitinib	Selleckchem	0.995	0.001	1.033	0.012	Multi-targeted RTK inhibitor
RXDX-106 (CEP-40783)	Selleckchem	0.995	0.006	0.888	0.008	TYRO3, AXL, MER and MET
Crenolanib (CP-868596)	Selleckchem	0.995	0.001	0.974	0.001	PDGFRα/β
Silmitasertib (CX-4945)	Selleckchem	0.995	0.003	0.977	0.016	CK2 (casein kinase 2)
BLZ945	Selleckchem	0.995	0.003	1.051	0.004	CSF-1R
Thalidomide	Selleckchem	0.996	0.008	0.922	0.003	E3 ubiquitin ligase
CCG 50014	Selleckchem	0.996	0.008	0.977	0.008	RGS4
ON123300	Selleckchem	0.997	0.001	0.901	0.004	Multi-targeted kinase
RK-33	Selleckchem	0.997	0.005	0.986	0.012	DDX3 (a RNA helicase)
TIC10 Analogue	Selleckchem	0.997	0.001	1.017	0.006	TRAIL
Verteporfin	Selleckchem	0.997	0.001	0.880	0.005	TEAD–YAP association
Sotrastaurin	Selleckchem	0.997	0.001	0.997	0.006	pan-PKC
ML264	Selleckchem	0.998	0.006	0.981	0.014	Kruppel-like factor 5 (KLF5)
BI3802	Boehringer Ingelheim	0.999	0.011	0.869	0.004	BCL6 degrader
Crizotinib	Selleckchem	1.000	0.007	0.938	0.012	ALK, MET, ROS1
Ferrostatin-1 (Fer-1)	Selleckchem	1.002	0.001	1.277	0.014	Ferroptosis inhibitor
ORY-1001	Selleckchem	1.003	0.011	0.666	0.017	LSD1/KDM1A
BI9627	Boehringer Ingelheim	1.003	0.006	1.003	0.006	NHE1
PF-3644022	Sigma-Aldrich	1.004	0.003	0.988	0.005	MAPK-activated protein kinase-2
BI3812	Boehringer Ingelheim	1.004	0.007	0.990	0.004	BCL6 inhibitor
Dipyridamole	Selleckchem	1.006	0.005	0.992	0.014	Phosphodiesterase
BMS-345541	Selleckchem	1.006	0.013	1.010	0.006	IKK-2 and IKK-1
RBC8	Selleckchem	1.006	0.007	0.973	0.006	RalA and RalB
Mechlorethamine	Selleckchem	1.007	0.008	0.983	0.013	Alkylating agent
Aripiprazole	Selleckchem	1.007	0.005	1.039	0.003	5-HT receptor partial agonist
Epacadostat	Selleckchem	1.007	0.013	1.159	0.016	IDO1
GSK269962A	Selleckchem	1.009	0.004	1.086	0.002	ROCK
BI99179	Boehringer Ingelheim	1.009	0.001	1.006	0.016	FAS
SF2523	Selleckchem	1.010	0.010	0.993	0.006	PI3Kα/γ, DNA-PK, BRD4, mTOR
Staurosporine	Selleckchem	1.011	0.004	0.981	0.011	PKCα, PKCγ and PKCη
Brigatinib (AP26113)	Selleckchem	1.011	0.012	1.023	0.002	ALK and ROS1

RSL3	Selleckchem	1.012	0.001	0.873	0.012	Ferroptosis activator
Wortmannin	Sigma-Aldrich	1.013	0.006	0.977	0.006	PI3K
Vinorelbine Tartrate	Selleckchem	1.015	0.004	1.381	0.001	Tubulin
OTX015	Selleckchem	1.019	0.011	0.890	0.016	BETi bromodomain
LOXO-101	Selleckchem	1.019	0.001	0.884	0.014	pan-TRK
SN-38	Selleckchem	1.021	0.001	1.048	0.011	DNA topoisomerase I
Fenofibrate	Selleckchem	1.024	0.005	0.949	0.001	PPAR agonist
XMD8-92	Selleckchem	1.037	0.008	0.913	0.006	ERK5
AI-10-49	Selleckchem	1.038	0.002	1.019	0.004	CBFβ-SMMHC/RUNX1 binding inhibitor
JWG-071	Gray Lab	1.038	0.005	1.053	0.006	ERK5
SP600125	Selleckchem	1.039	0.008	0.867	0.006	JNK
CPI-0610	Selleckchem	1.040	0.003	0.785	0.013	BETi bromodomain
Palbociclib (PD-0332991)	Selleckchem	1.045	0.004	1.170	0.011	CDK4/6
Linsitinib (OSI-906)	Selleckchem	1.047	0.008	0.868	0.005	IGF-1R
BI1347	Boehringer Ingelheim	1.048	0.001	1.093	0.016	CDK8
PTC-209	Selleckchem	1.048	0.008	1.101	0.004	BMI1
Everolimus	Selleckchem	1.048	0.007	1.248	0.009	mTOR
Poziotinib	Selleckchem	1.051	0.004	0.920	0.006	HER1/2/4
Celecoxib	Selleckchem	1.055	0.014	0.988	0.015	COX2 inhibitor
TH588	Selleckchem	1.057	0.004	1.084	0.002	MTH1 (NUDT1)
Nutlin-3	Selleckchem	1.064	0.004	0.997	0.001	MDM2
BGJ398 (NVP-BGJ398)	Selleckchem	1.064	0.008	1.012	0.014	FGFR1/2/3
Plinabulin (NPI-2358)	Selleckchem	1.064	0.001	1.102	0.009	VDA
Defactinib (PF-04554878)	Selleckchem	1.066	0.002	0.961	0.002	FAK
MK-2206	Selleckchem	1.066	0.004	1.012	0.007	Akt1, Akt2 and Akt3
MRT68921	Selleckchem	1.066	0.001	1.105	0.013	ULK1/2
GSK481	Selleckchem	1.069	0.006	1.123	0.008	RIP1
JIB-04	Selleckchem	1.072	0.011	0.633	0.012	pan-Jumonji histone demethylase
Selinexor (KPT-330)	Selleckchem	1.074	0.016	1.016	0.013	CRM1/Xpo1
Dactolisib (BEZ235)	Selleckchem	1.085	0.007	0.896	0.008	PI3K and mTOR
SBI-0640756	Selleckchem	1.089	0.006	0.961	0.015	eIF4G1
BY1002494	Boehringer Ingelheim	1.103	0.004	1.047	0.005	SYK
GMX1778 (CHS828)	Selleckchem	1.106	0.008	1.157	0.001	NAMPT
Dorsomorphin	Selleckchem	1.109	0.002	1.085	0.004	AMPK
Milciclib (PHA-848125)	Selleckchem	1.114	0.009	1.219	0.011	CDK2
Tipiracil hydrochloride	Selleckchem	1.114	0.010	1.200	0.015	Thymidine phosphorylase
Luminespib (AUY-922)	Selleckchem	1.114	0.013	1.301	0.014	HSP90α/β

Entinostat (MS-275)	Selleckchem	1.128	0.004	0.753	0.011	HDAC1 and HDAC3
LY3214996	Selleckchem	1.129	0.013	1.112	0.007	ERK1/2
VLX1570	Selleckchem	1.148	0.013	1.011	0.010	USP14
eFT-508	Selleckchem	1.149	0.008	1.153	0.003	MNK1/2
SHP099 dihydrochloride	Selleckchem	1.150	0.002	0.965	0.009	SHP2
Daporinad (FK866)	Selleckchem	1.150	0.002	1.147	0.015	NMPRT
Hydroxychloroquine	Selleckchem	1.154	0.011	1.039	0.012	Autophagy
URMC-099	Selleckchem	1.158	0.001	1.003	0.011	MLK
SB743921	Selleckchem	1.160	0.001	0.706	0.012	Kinesin spindle protein (KSP)
Bortezomib	Selleckchem	1.163	0.012	0.767	0.001	20S proteasome
Entrectinib (RXDX-101)	Selleckchem	1.163	0.010	0.989	0.003	pan-TrkA/B/C, ROS1 and ALK
CBL0137	Selleckchem	1.169	0.007	1.119	0.013	NF-kB
MRT67307	Selleckchem	1.173	0.012	1.107	0.015	IKKε and TBK1
Barasertib (AZD1152)	Selleckchem	1.173	0.004	1.109	0.016	Aurora B
Erlotinib	Selleckchem	1.173	0.001	1.116	0.012	EGFR
Vorinostat	Selleckchem	1.181	0.011	0.805	0.007	HDAC
Alisertib (MLN8237)	Selleckchem	1.181	0.004	1.102	0.004	Aurora A
Doramapimod	Selleckchem	1.181	0.006	1.267	0.015	MAPK14
PLX7904	Selleckchem	1.182	0.007	1.203	0.016	RAF
BAY 11-7082	Selleckchem	1.183	0.004	1.305	0.008	NF-κB
Dasatinib	Selleckchem	1.203	0.006	0.856	0.012	Abl, Src and c-Kit
LY3009120	Selleckchem	1.205	0.002	1.100	0.013	pan-Raf
Ulixertinib (BVD-523)	Selleckchem	1.213	0.013	1.017	0.017	ERK1/ERK2
Fluorouracil (5-FU)	Selleckchem	1.222	0.011	1.363	0.016	Thymidylate synthase
SCH772984	Selleckchem	1.234	0.005	1.123	0.001	ERK1/2
AZD5153	Selleckchem	1.263	0.001	0.819	0.003	BETi bromodomain
MSC2530818	Selleckchem	1.275	0.008	1.227	0.001	CDK8
XMD16-5	Selleckchem	1.280	0.021	1.104	0.004	TNK2
BQU57	Selleckchem	1.285	0.020	1.167	0.016	GTPase Ral
CPI-455 HCl	Selleckchem	1.295	0.013	1.237	0.006	KDM5
BI 2536	Selleckchem	1.317	0.006	0.561	0.016	PLK1
Erastin	Selleckchem	1.322	0.005	1.197	0.009	Ferroptosis activator
Vildagliptin (LAF-237)	Selleckchem	1.340	0.021	1.122	0.007	DPP−4
Volasertib (BI 6727)	Selleckchem	1.361	0.021	0.863	0.011	PLK1, PLK2 and PLK3
BI2536	Boehringer Ingelheim	1.377	0.014	0.613	0.006	PLK1
XMU-MP-1	Selleckchem	1.391	0.004	1.411	0.005	MST1/2
Cyclophosphamide	Selleckchem	N/A	N/A	1.478	0.005	Alkylating agent

Supplementary Table S2. List of potential SMYD3 substrates identified by biochemical protein array screen. Proteins in grey are predicted false positives with potential auto-methylation activity.

Gene ID	Official Symbol	Official Full Name
55114	ARHGAP17	Rho GTPase activating protein 17
136991	ASZ1	Ankyrin repeat, SAM and basic leucine zipper domain-containing protein 1
138199	CARNMT1	Carnosine N-methyltransferase 1
23059	CLUAP1	Clusterin associated protein 1
1312	COMT	Catechol-O-methyltransferase
10987	COPS5	COP9 signalosome subunit 5
151194	METTL21a	Methyltransferase like 21A
4000	LMNA	Lamin A/C
51451	LCMT1	Leucine carboxyl methyltransferase 1
10746	MAP3K2	Mitogen-activated protein kinase kinase kinase 2
26155	NOC2L	NOC2 like nucleolar associated transcriptional repressor
4869	NPM1	Nucleophosmin 1
27445	PCLO	Piccolo presynaptic cytomatrix protein
5110	PCMT1	Protein-L-isoaspartate(D-aspartate) O-methyltransferase
5303	PIN4	Peptidylprolyl cis/trans isomerase, NIMA-interacting 4
3276	PRMT1	Protein arginine N-methyltransferase 1
55170	PRMT6	Protein arginine N-methyltransferase 6
56341	PRMT8	Protein arginine N-methyltransferase 8
83732	RIOK1	RIO kinase 1
7737	RNF113A	Ring finger protein 113A
56950	SMYD2	SET and MYND domain-containing protein 2
6672	SP100	SP100 nuclear antigen

Supplementary Table S3: List of identified proteins binding to RNF113A-K20me0 and RNF113A-K20me3 peptides in the peptide-pulldown quantitative proteomics analysis. Two independent experiments using forward (Heavy: RNF113A-K20me3, Light: RNF113A-K20me0) and reverse (Heavy: RNF113A-K20me0, Light: RNF113A-K20me3) labeling were performed.

Table provided in a separate .xls file.

Supplementary Table S4. List of RNF113A phosphorylated sites collected from PhosphoSitePlus database and in-house identification by 2 independent mass spectrometry analyses of RNF113A purified from HeLa cells. Sites in grey are potential substrates for the Serine/Threonine PP4 phosphatase.

RNF113A phosphorylated sites	PhosphoSitePlus HTP records	Peptide sequences identified by LC-MS in this study
S6	14	EPIQSTGSMAEQLSPGK
S43	2	
S45	4	
S46	3	RPACDPEPGESGSSSDEGCTVVRPEK
S47	2	
Y80	9	
S84	50	AAYGDLSSEEEEENEPESLGVVYK
S85	50	
Y120	10	
T124	1	
Y153	52	
Y159	4	
Y162	1	
T168	2	
S169	3	
S174	1	
S175	2	
T192	1	
Y244	1	
Y249	4	
S253	52	YGVYEDENYEVGSDDEEIPFK
S268	1	
T323	1	
S329	6	ATGEGGASDLPEDPDEDAIPIT

Supplementary Table S5. Graphical representations of immunoblots quantification from the study. Calculation was performed using Image J software comparing the integrated density of immunoblot signals using at least three different exposures. Background was subtracted and when relevant, signal was normalized with proper references (total protein level, level of immunoprecipitated protein, control, untreated condition, …).

Figure 3

Panel A

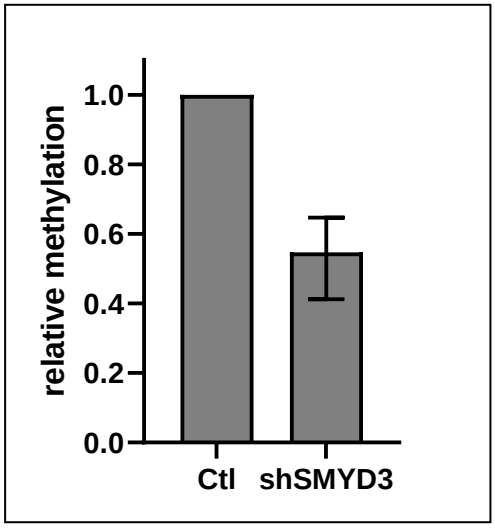

Panel B

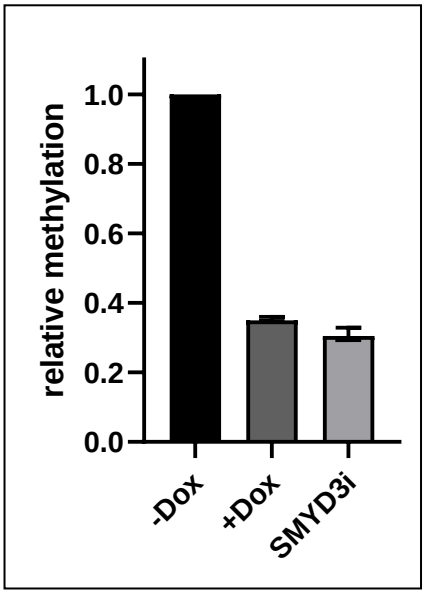

Figure 4

Panel E

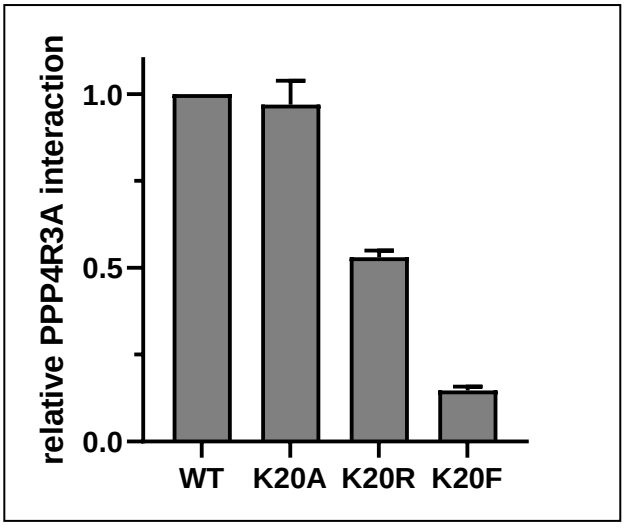

Panel I

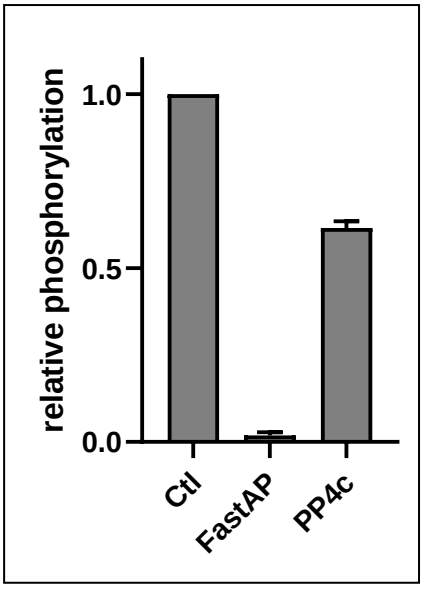

Figure 5

Panel A

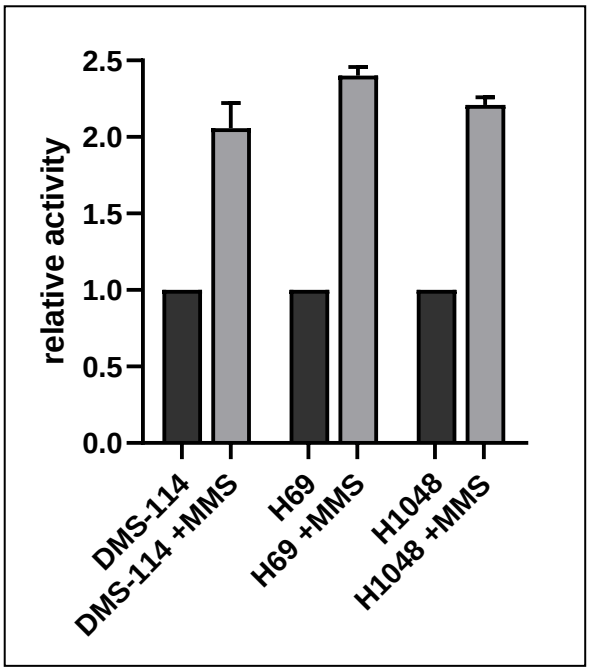

Panel B

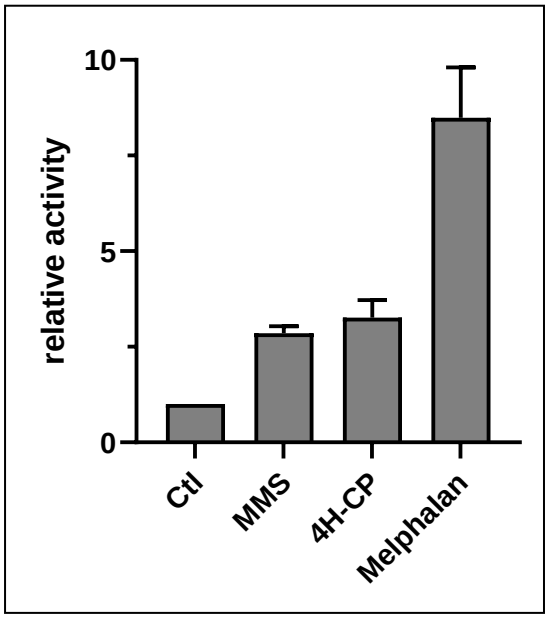

Panel C

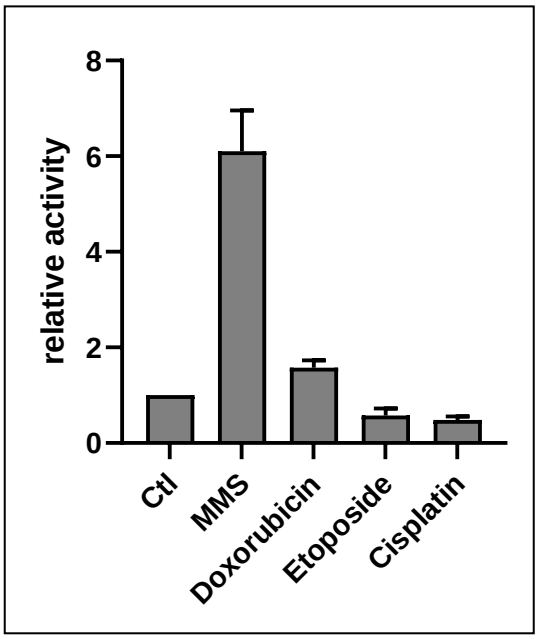

Panel D

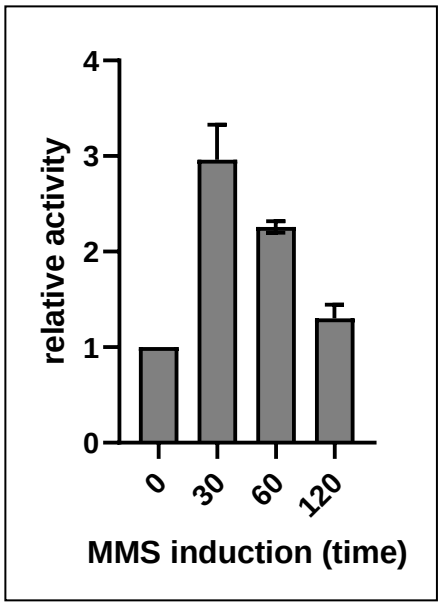

Panel E

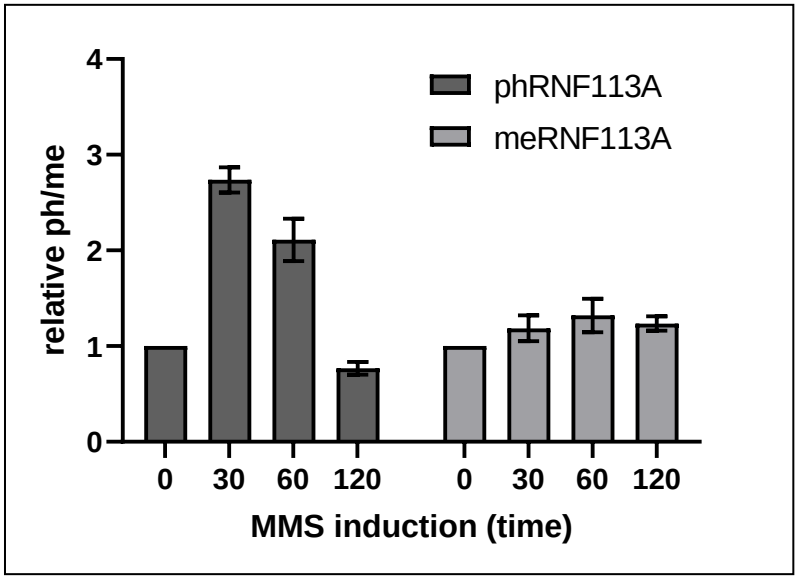

Panel F

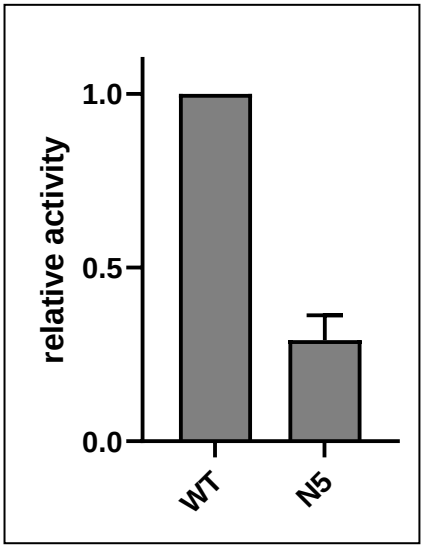

Panel G

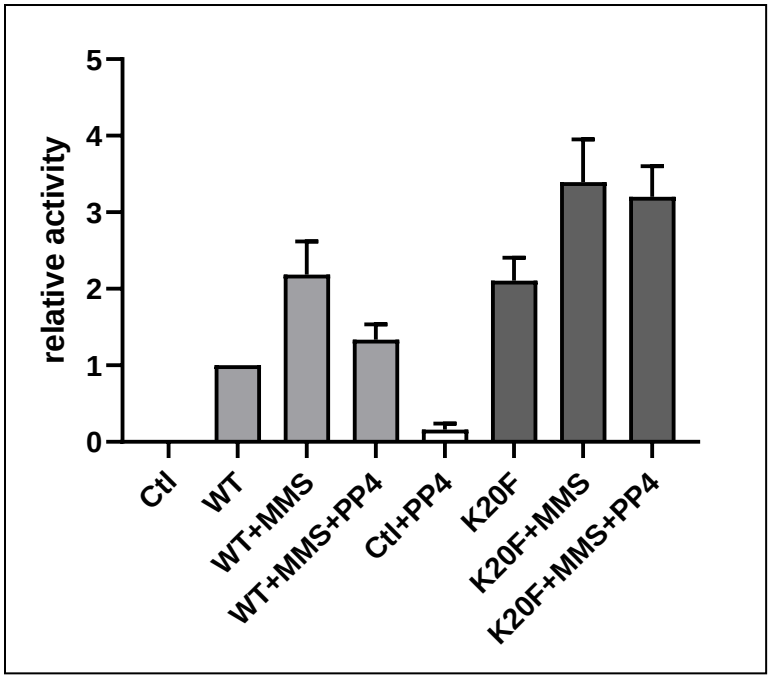

Figure 6

Panel F

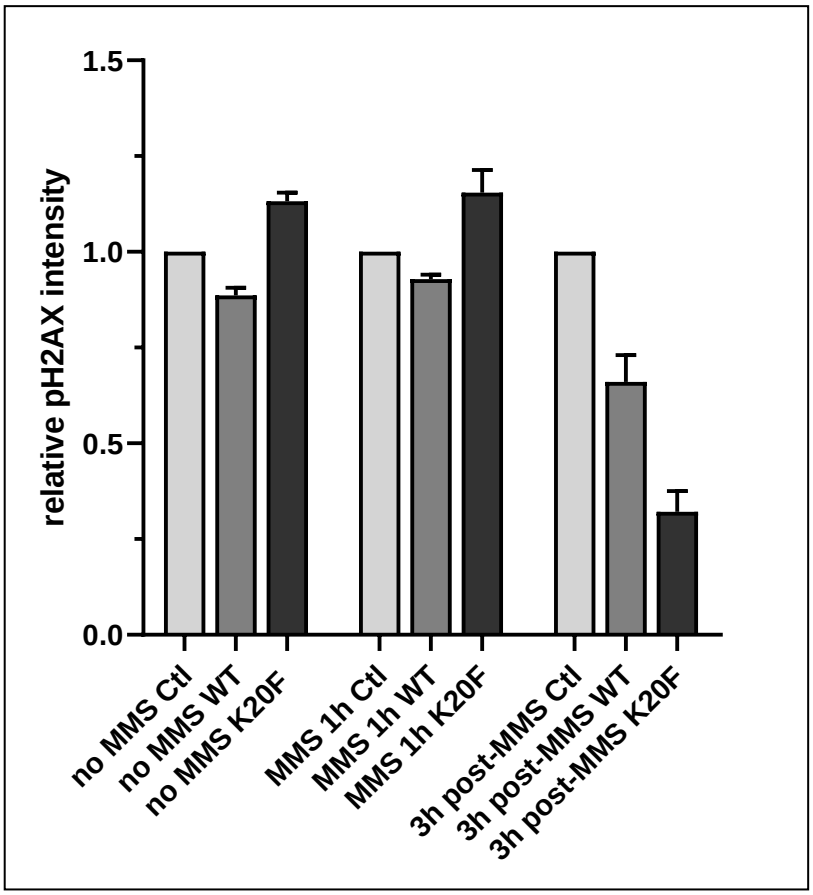

Figure 7

Panel B

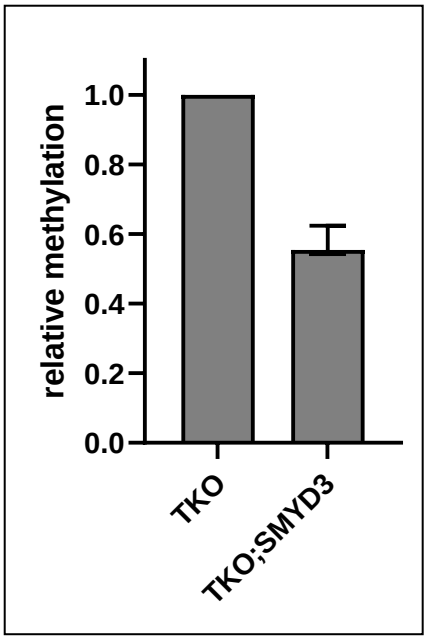

Figure S2

Panel A

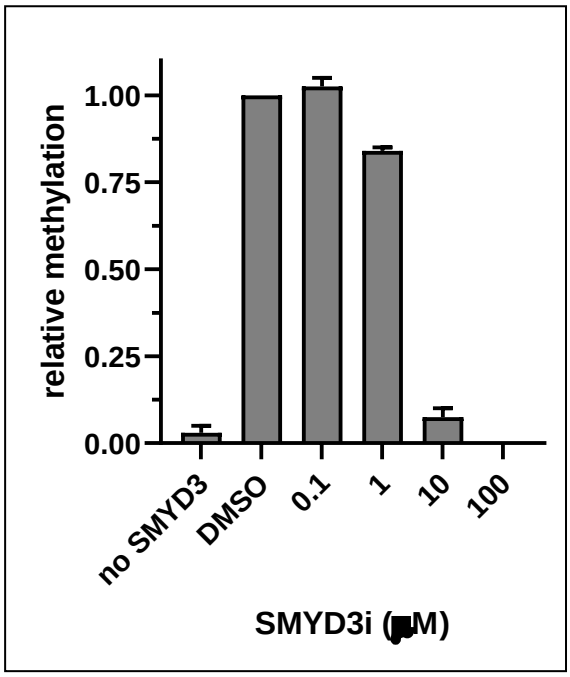

Figure S3

Panel A

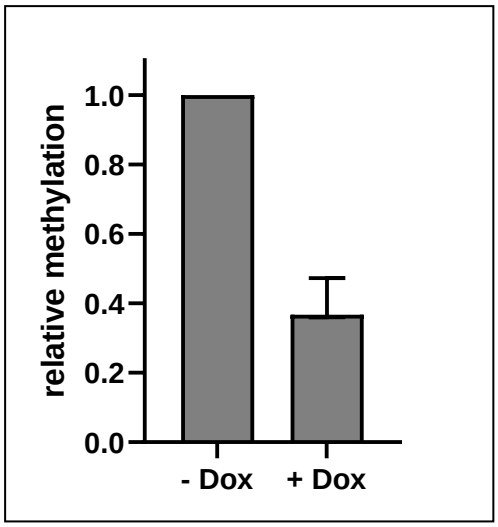

Panel B

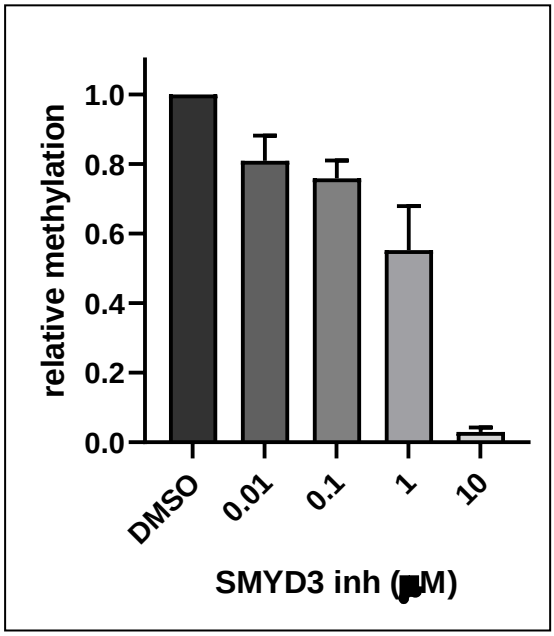

Figure S4

Panel A

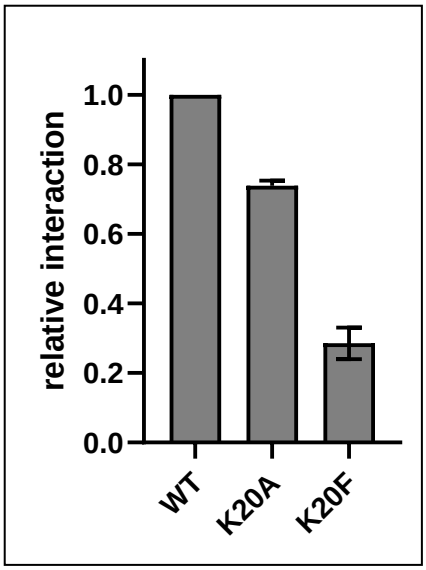

Figure S5

Panel B

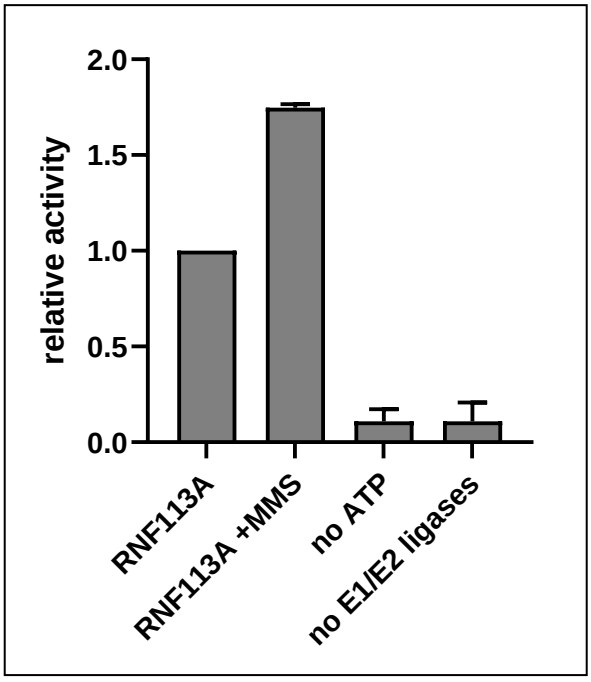

Panel C

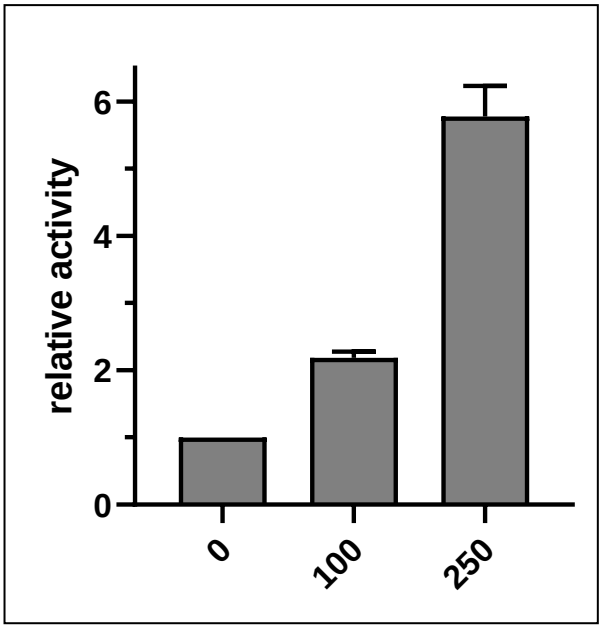

Panel D

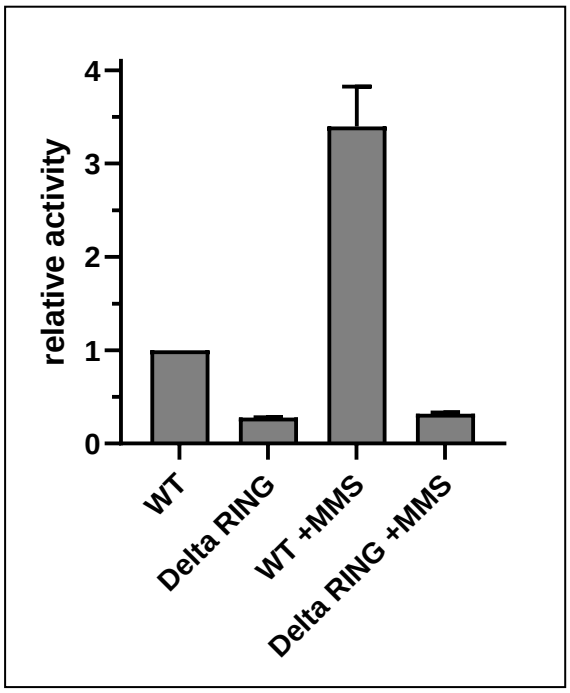

Panel E

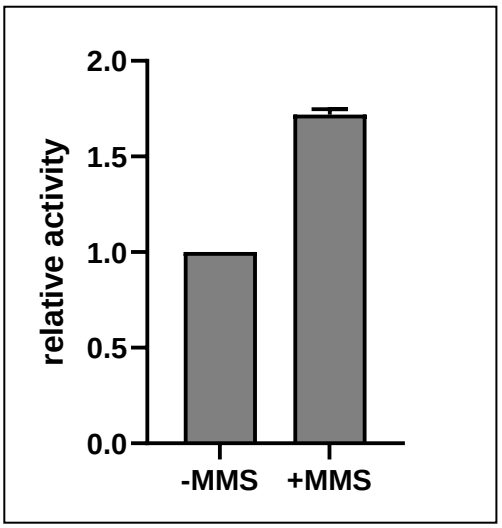

Panel G

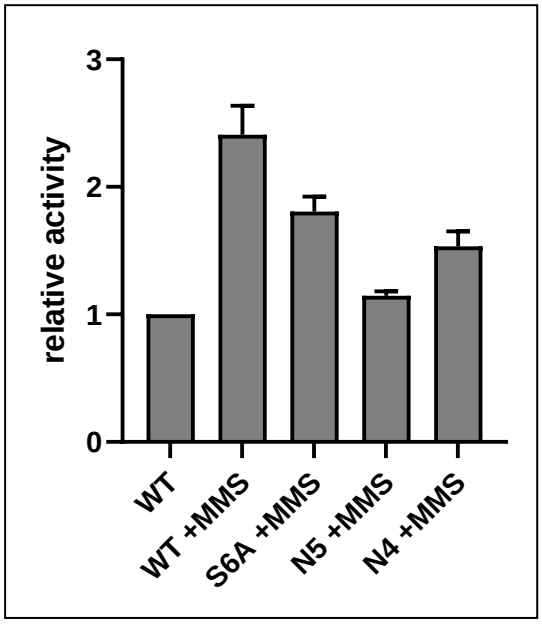

Panel H

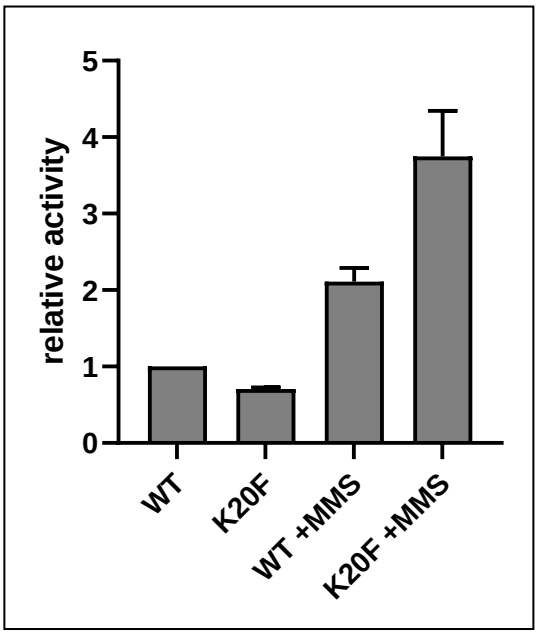

Panel I

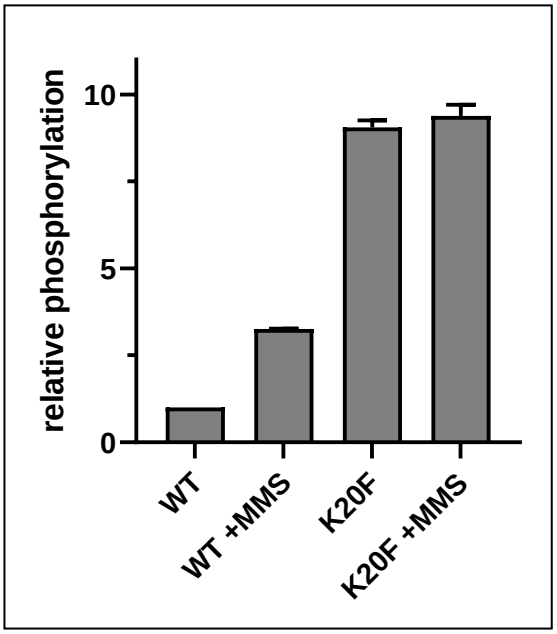

Panel J

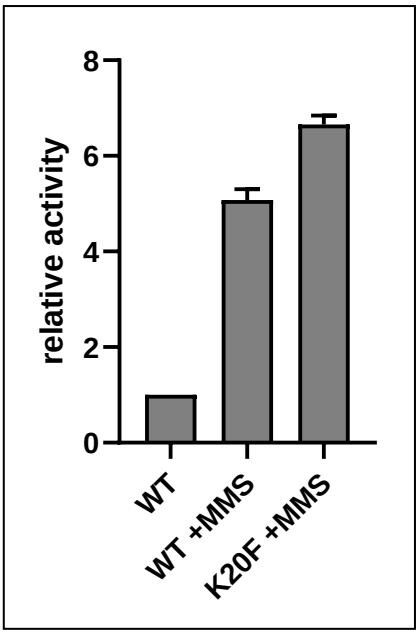

Panel K

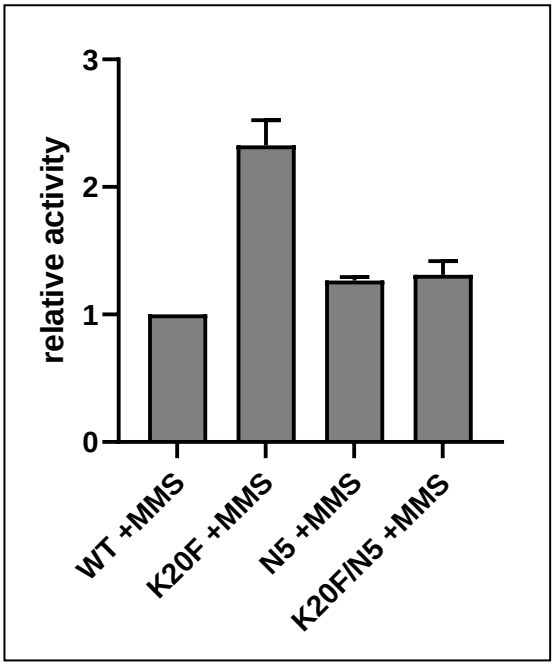

Supplementary References

Bouyssié D, Hesse A-M, Mouton-Barbosa E, Rompais M, Macron C, Carapito C, Gonzalez de Peredo A, Couté Y, Dupierris V, Burel A, *et al* (2020) Proline: an efficient and user-friendly software suite for large-scale proteomics. *Bioinformatics* 36: 3148–3155

Brickner JR, Soll JM, Lombardi PM, Vågbø CB, Mudge MC, Oyeniran C, Rabe R, Jackson J, Sullender ME, Blazosky E, *et al* (2017) A ubiquitin-dependent signalling axis specific for ALKBH-mediated DNA dealkylation repair. *Nature* 551: 389–393

Chu VT, Weber T, Graf R, Sommermann T, Petsch K, Sack U, Volchkov P, Rajewsky K & Kühn R (2016) Efficient generation of Rosa26 knock-in mice using CRISPR/Cas9 in C57BL/6 zygotes. *BMC Biotechnol* 16: 4

Cox J & Mann M (2008) MaxQuant enables high peptide identification rates, individualized p.p.b.-range mass accuracies and proteome-wide protein quantification. *Nat Biotechnol* 26: 1367–1372

Fushiki H, Kanoh-Azuma T, Katoh M, Kawabata K, Jiang J, Tsuchiya N, Satow A, Tamai Y & Hayakawa Y (2009) Quantification of mouse pulmonary cancer models by microcomputed tomography imaging. *Cancer Sci* 100: 1544–1549

Jonkers J, Meuwissen R, van der Gulden H, Peterse H, van der Valk M & Berns A (2001) Synergistic tumor suppressor activity of BRCA2 and p53 in a conditional mouse model for breast cancer. *Nat Genet* 29: 418–425

Levy D, Liu CL, Yang Z, Newman AM, Alizadeh AA, Utz PJ & Gozani O (2011) A proteomic approach for the identification of novel lysine methyltransferase substrates. *Epigenetics Chromatin* 4: 19

Lim JS, Ibaseta A, Fischer MM, Cancilla B, O'Young G, Cristea S, Luca VC, Yang D, Jahchan NS, Hamard C, *et al* (2017) Intratumoural heterogeneity generated by Notch signalling promotes small-cell lung cancer. *Nature* 545: 360–364

Liu S, Hausmann S, Carlson SM, Fuentes ME, Francis JW, Pillai R, Lofgren SM, Hulea L, Tandoc K, Lu J, *et al* (2019) METTL13 Methylation of eEF1A Increases Translational Output to Promote Tumorigenesis. *Cell* 176: 491-504.e21

Mazur PK, Reynoird N, Khatri P, Jansen PWTC, Wilkinson AW, Liu S, Barbash O, Van Aller GS, Huddleston M, Dhanak D, *et al* (2014) SMYD3 links lysine methylation of MAP3K2 to Ras-driven cancer. *Nature* 510: 283–287

Nakada S, Chen GI, Gingras A-C & Durocher D (2008) PP4 is a gamma H2AX phosphatase required for recovery from the DNA damage checkpoint. *EMBO Rep* 9: 1019–1026

Raymond CS & Soriano P (2007) High-efficiency FLP and PhiC31 site-specific recombination in mammalian cells. *PLoS ONE* 2: e162

Schaffer BE, Park K-S, Yiu G, Conklin JF, Lin C, Burkhart DL, Karnezis AN, Sweet-Cordero EA & Sage J (2010) Loss of p130 accelerates tumor development in a mouse model for human small-cell lung carcinoma. *Cancer Res* 70: 3877–3883

Skarnes WC, Rosen B, West AP, Koutsourakis M, Bushell W, Iyer V, Mujica AO, Thomas M, Harrow J, Cox T, *et al* (2011) A conditional knockout resource for the genome-wide study of mouse gene function. *Nature* 474: 337–342

Tyanova S, Temu T, Sinitcyn P, Carlson A, Hein MY, Geiger T, Mann M & Cox J (2016) The Perseus computational platform for comprehensive analysis of (prote)omics data. *Nat Methods* 13: 731–740

Wang X, Finegan KG, Robinson AC, Knowles L, Khosravi-Far R, Hinchliffe KA, Boot-Handford RP & Tournier C (2006) Activation of extracellular signal-regulated protein kinase 5 downregulates FasL upon osmotic stress. *Cell Death Differ* 13: 2099–2108